1) ~~Smith~~
2) File

1965B
A-51255-AA-1A

INVESTIGATION OF THIN DIELECTRIC FILMS FOR ENERGY CONVERSION

Quarterly Report No. 3

15 March 1965

Contract No. NAS 2-1995
Contract Supervisor: Benjamin H. Beam
Westinghouse Reference AAD-51255

Prepared for

AMES RESEARCH CENTER
National Aeronautics and Space Administration
Moffett Field, California

By

WESTINGHOUSE ELECTRIC CORPORATION
Aerospace Division
Baltimore, Maryland

ABSTRACT

Energy conversion by the thermoelectrostatic effect has been demonstrated by experimental output-input energy ratios of up to 2.22 using composite film thermoelectrostatic samples in the modified energy conversion circuit designed by the sponsor. Output and input energies were computed from the changes in voltages of calibrated temperature-stable condensers (in room ambient, not in the sample environment) which were used as source and output storage condensers respectively. The capacitance of the thermoelectrostatic working condenser was less than 1/20th of that of source or output condenser.

Capacitance measurements as a function of temperature were made on a number of homogeneous and composite dielectric films with the low-frequency capacitance bridge specially constructed for this project. Additional curves are given for certain homogeneous films and for the teflon-mylar sandwiches of both types. As distinguished from the behavior of homogeneous films, the composite films show significant capacitance change just above and just below room temperature ambient, and also in the lower temperature ranges achievable with a new environmental chamber cooled with CO_2 from a tank.

A new phenomenon in single and composite films, namely a thermally generated voltage, has been discovered, and can be utilized to increase the energy conversion significantly. The effect has been shown to be real, characteristic of a particular sample, and to survive both subjection to a vacuum of 5×10^{-5} torr, and storage. For these and other reasons discussed in the report, the effect is not the result of an air film contained between the halves of the composite. The thermally generated voltages in homogeneous samples tend to be smaller than those in composite samples, but still significant.

A derivation is made of the energy conversion ratio to be expected for the thermoelectrostatic cycle, in terms of measurable experimental parameters. This derivation permits choice of suitable materials and dielectric constant

ratios, while at the same time avoiding cycles which will place undesirably high voltages on the condenser dielectrics. Details of these and other work results are given more fully in the text.

Certain of the desirable directions of further investigation for maximization of the efficiency and progress toward working thermoelectrostatic energy converters have been considered.

TABLE OF CONTENTS

LIST OF ILLUSTRATIONS

LIST OF TABLES

1. INTRODUCTION

The thermoelectrostatic energy conversion cycle[1, 2, 3] converts solar energy to electrical energy through the effect of heating or cooling of the charged dielectric of a condenser. During the quarter just completed, a number of additional plastic films have been prepared as condensers and measured in the thermoelectrostatic cycle, including both thin-films of single materials and composite thin-films.

At the temperatures used initially, many of the materials which showed the most favorable change of dielectric constant with temperature, also showed undesirable high values of electrical leakage; also, a number of materials were found which had high internal resistance but negligible change of dielectric constant with temperature. To utilize the favorable properties of both types of materials, composite thin-film condensers have been fabricated using one of each type of material; one yields the desired change of dielectric constant, and the other prevents leakage loss of the electrical energy generated in the cycle.

In a number of samples of one composite dielectric, a pyroelectric type behavior was observed; it has been possible to use this to enhance the energy conversion. This is an extended thermoelectrostatic cycle, since the conversion of solar energy to electrical energy is caused by the heating and cooling of the dielectric, and conversion requires the circuit and the switching steps described in references 1 through 3. However, instead of output energy to input energy ratios of 1.0 to 1.3, it has been possible to obtain ratios of up to 2.22.

This new phenomenon which enhances the efficiency of the thermoelectrostatic cycle, the ranges and limits thereto, the measurements made on other materials, the initial testing under vacuum, and the energy conversion ratio to be expected from the thermoelectrostatic cycle using materials with given thermoelectrostatic parameter values are the topics discussed in this report.

2. ENERGY CONVERSION MEASUREMENT TECHNIQUES AND ENERGY RATIOS

2.1 THE THERMOELECTROSTATIC ENERGY CONVERSION CIRCUIT OF B.H. BEAM

2.1.1 Circuit Schematic

The circuit of figure 2-1, with a suitable switching and heating cycle, makes possible high-efficiency, continuous solar energy conversion in a rotating satellite.

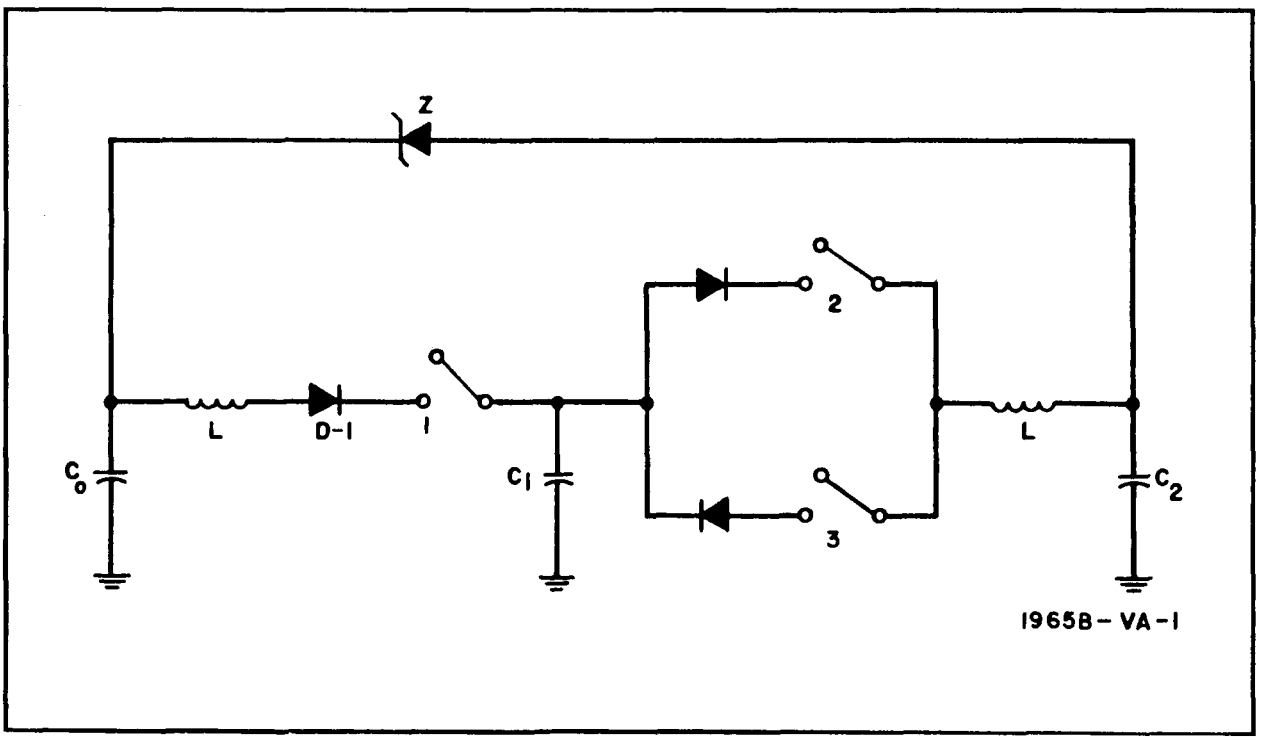

Figure 2-1. Thermoelectrostatic Energy Conversion Circuitry

2.1.2 Energy Conversion Cycle

The working thermoelectrostatic element is the condenser C_i. At the commencement of the cycle, assume (without loss of generality) that its

voltage is less than that across C_0. For this example, assume that the initial voltage across C_0 equals that across C_2.

a. Close and then open switch 1. C_i receives charge from C_0, and a corresponding amount of energy.

b. Change the temperature of C_i so as to decrease the dielectric constant of its dielectric. The voltage across C_i rises, and its energy content increases.

c. Close and then open switch 2. Charge and energy flow from C_i onto C_2.

d. Bring C_i back to its original temperature. Its voltage and energy content decrease. Its voltage is below that of C_0, and the voltage of C_0 is obviously below that of C_2.

e. Close and open switch 1. C_i receives additional charge and energy from C_0.

f. Close and open switch 3. C_i receives a small additional amount of charge and energy from C_2; this is less than that delivered to C_2 in step c.

g. Change the temperature of C_i to decrease its dielectric constant. Voltage and energy content increase, with final voltage greater than that of C_2.

h. Close and open switch 2. Charge and energy flow from C_i to C_2.

By repetition of steps d to h inclusive, charge is taken from C_0 and transferred to C_2 at a higher and higher voltage level, and therefore with a greater and greater energy content.

2.1.3 Circuit Details

C_0 is the source condenser, C_i the working thermoelectrostatic condenser, and C_2 the storage condenser. Since charge must be returned to C_0, the load preferably should be placed across Z. When the voltage across the zener diode ($V_2 - V_0$) is less than Z, the thermoelectrostatic cycle builds up the voltage in C_2. When it exceeds Z, charge bleeds back to C_0 and is available for continued solar energy conversion; the cycle maintains the difference $V_2 - V_0 = Z$.

An inductance is shown in series with the diode in the branch from C_0 to C_i. This will decrease energy loss in the transfer of charge in steps a, e, and subsequent steps of type e. The advantage offered by it must be coordinated with the weight penalty before the decision is finally made as to whether to include it.

Although $C_2 - C_0$ never exceeds Z, the individual voltages of C_0, C_i, and C_2 will build up with respect to ground as the cycle progresses. Dielectric breakdown from this cause can be avoided by including a zener diode of proper characteristics (or several in series) in parallel with C_i, across its two surfaces.

2.1.4 Laboratory Measurement Circuit and Cycles

2.1.4.1 Measurement Circuit

In the present measurements, the circuit of figure 2-1 was used, with the omission of the first inductance and the branch containing the zener diode, since the primary aim was to determine energy ratios and not continuous energy production. Energy input was computed from the voltages and capacitance of C_0, and energy output by the voltages and capacitance of C_2. Both C_0 and C_2 are precision capacitors.

2.1.4.2 Technique Modifications to Provide for Either Sign of Applied Voltage

Figure 2-1 shows the circuit and paragraph 2.1.2 describes the switching and heating cycle when the capacitors are charged positively with respect to ground.

Because of the phenomenon described in Appendix A, it was desirable to compare results, as well, when the capacitors were charged negatively. When this was done, the diode D-1 was reversed; where in paragraph 2.1.2 the technique calls for closing of switch 2, switch 3 was closed, and where the technique calls for closing switch 3, switch 2 was closed. This modified cycle transfers negative charge onto C_2; energy transfer is analogous to that previously described.

2.2 ENERGY RATIO

2.2.1 Definition

The energy conversion is described in this report by the ratio, R_1, of the energy output into C_2 from C_i after the solar irradiation cycle, to that initially put into C_i from C_0. In the steady state, for which the ratio is computed, C_i has the same voltage at the end of each cycle (e.g., the steps d to h in paragraph 2.1.2). There was also computed the ratio, R_2, total energy content of the system before and after a number of thermoelectrostatic cycles. Because of the stored energy in C_i, this ratio was somewhat less than C_1; capacitance values of C_i were of the order of 1/20th of C_0 or C_2, so that values of R_1 significantly greater than one always implied significantly greater than one values of R_2. To the user, or to the space vehicle, the important parameter is the output-input ratio, and not R_2. In the design phase, it may be desirable to consider both ratios, since a comparison of the two indicates the overall energy content necessary for a given output-input energy ratio.

In Appendix B, the measurable output-input energy ratio for given circuit parameters and materials characteristics is calculated.

2.2.2 Energy Losses

In the experiments reported here, no inductance was included in the circuit between C_0 and C_i. Therefore, there was a sizeable switching loss in the transfer when switch 1 is closed. Values of energy conversion given below have not been corrected for this energy loss, so that if optimum conditions had been used, higher ratios would have been obtained.

Energy losses also are suffered from leakage in C_i (leakage in the precision condensers is negligible), and from the backward current in the diodes (which continually abstracts energy and feeds it in the reverse direction). Energy loss of the I^2R type is also suffered. None of these energy losses have been corrected for. Therefore, in an optimally designed prototype, higher values of R_1 will be obtained than the ones measured here with the same materials.

2.2.3 The Energy Conversion Ratio and Its Calculation

The energy conversion ratio, R_1, defined above, is:

$$R_1 = \frac{\Delta E_2}{-\Delta E_0} = \frac{\text{Energy output into } C_2}{\text{Energy input from } C_0} = \frac{C_2 (V_{2f}^2 - V_{20}^2)}{C_0 (V_{00}^2 - V_{0f}^2)} \qquad (2\text{-}1)$$

The energy conversion ratio, R_2, defined above is:

$$R_2 = \frac{(E_0 + E_i + E_2)_f}{(E_0 + E_i + E_2)_0} = \frac{\text{Total final energy content}}{\text{Total initial energy content}}$$

$$= \frac{(C_0 V_0^2 + C_i V_i^2 + C_2 V_2^2)_f}{(C_0 V_0^2 + C_i V_i^2 + C_2 V_2^2)_0}$$

As described in Appendix C, determination of energy contents by the voltages and capacitances of the condensers provides unambiguous proof of energy conversion; it avoids any errors which may result from methods such as first tried and reported in the first quarterly, namely thermocouple, gas thermometer, bolometer, etc, and avoids any difficulties with energy integration.

3. COMPOSITE DIELECTRICS FOR ENERGY CONVERSION

3.1 REASON FOR COMPOSITE SAMPLES

At the temperatures at which measurements were made on the samples reported in the second quarterly report, a tendency was observed for samples of plastic film to be either highly resistant with negligible beta, or to have good beta and low internal resistance. Some few would be on the borderline in each. Composite samples were fabricated so as to combine the advantages of a plastic film with a good value of beta (and therefore energy conversion), with the resistive barrier between the electrodes which is furnished by the second, highly resistive film.

Lower temperature regions, as suggested by the sponsor, have shown better retention of resistivity in films with good beta. However, the composite films have shown the phenomenon described in Appendix A, which improves energy conversion.

3.2 FABRICATION OF COMPOSITE SAMPLES

Composite samples have been fabricated from various combinations of two materials. Various combining techniques have been used. These include: lamination in the strict sense, cementing together with plastic cement, cementing onto an aluminum ring and cementing of the second film to the first only over the cemented portion of the first.

Metal electrodes have been evaporated onto the opposite sides of these samples; masking provided a separation region on one side to eliminate surface leakage. Some materials were obtained with one side already metallized. Samples have been given annealing treatment where desirable, and all samples were given prolonged vacuum pumping before use.

4. ENERGY CONVERSION RATIOS, AND DEPENDENCE UPON SIGN OF CHARGING: EXPERIMENTAL

4.1 THERMAL CHAMBERS

In addition to the thermal chamber (oven) which had been used in the rough measurements reported in the second quarterly report, a precision thermal environmental chamber was used. This provided a working space of 10 by 10 by 7 inches, temperature control to 1/2 degree C, and temperature rate of change of 60°C down, or 70°C up in 2 minutes. The cooling was by liquid CO_2 from a tank, and the heating by internal heater. At the suggestion of the sponsor, this was modified so that heating could be rapid; the sun gun was introduced into the thermal chamber, the environment was maintained at the desired low temperature by CO_2 flow, and, when desired, the sample was raised in temperature by the sun gun. Sample temperatures were verified by measurement of dielectric properties under sun gun irradiation, and under controlled known temperature. By this method a change in temperature upwards of 100°C in 10 seconds was used, and even greater rates are possible.

In addition to the 3-inch-diameter dielectric samples, 8- by 8-inch and 7- by 7-inch samples were prepared and measured in the thermal chamber.

4.2 PRECISE DEPENDENCE OF DIELECTRIC CONSTANT UPON THE TEMPERATURE

With the new environmental chamber, temperature control was good enough so that the best precise temperature range for dielectric cycling could be used; because of the uniformity of temperature, no temperature-caused differences in dielectric constant over the area of the sample should be expected. Accordingly, a measurement with the low-frequency capacitance bridge was made of various samples to determine the temperature region of maximum

change of dielectric constant. Figure 4-1 shows sample curves of the dielectric constant dependence on temperature as measured with the low-frequency capacitance bridge, constructed for this work. The measurements were taken generally at 1 cps.

During the accumulation of this data, it was noticed that a number of composite samples exhibited a temperature hysteresis of dielectric constant.

4.3 THE QUASI-PYROELECTRIC EFFECT

The hysteresis was found to be not in the dielectric constant, but in a thermally generated voltage or charge (opposite charge on opposite sides of the sample dielectric). An example is shown in figure 4-2. The charge shows hysteresis, and the voltage may be computed from it by the capacitance of the dielectric. If the cycling is very slow (minutes), the charge decays by conduction, but if it is rapid (seconds or fractions of a second), the voltage on the condenser nearly follows the temperature change, linearly. Because of a finite time constant, if the sample is left undisturbed at any temperature for half an hour, the ambient temperature becomes the new zero of voltage, and the voltage is nearly proportional to the deviation of transiently (rapid) applied temperature from ambient. The turnover of the hysteresis curve determines the limiting value of the voltage obtainable by temperature excursion.

If the temperature cycling is not rapid, various apparently complex, and difficult to explain voltage variations are observed. With rapid cycling, (frequency > 1 cycle per minute) a relatively linear dependence on temperature can be obtained.

The effect is obtained to a lesser degree on homogeneous films, and to a greater degree on some composite films.

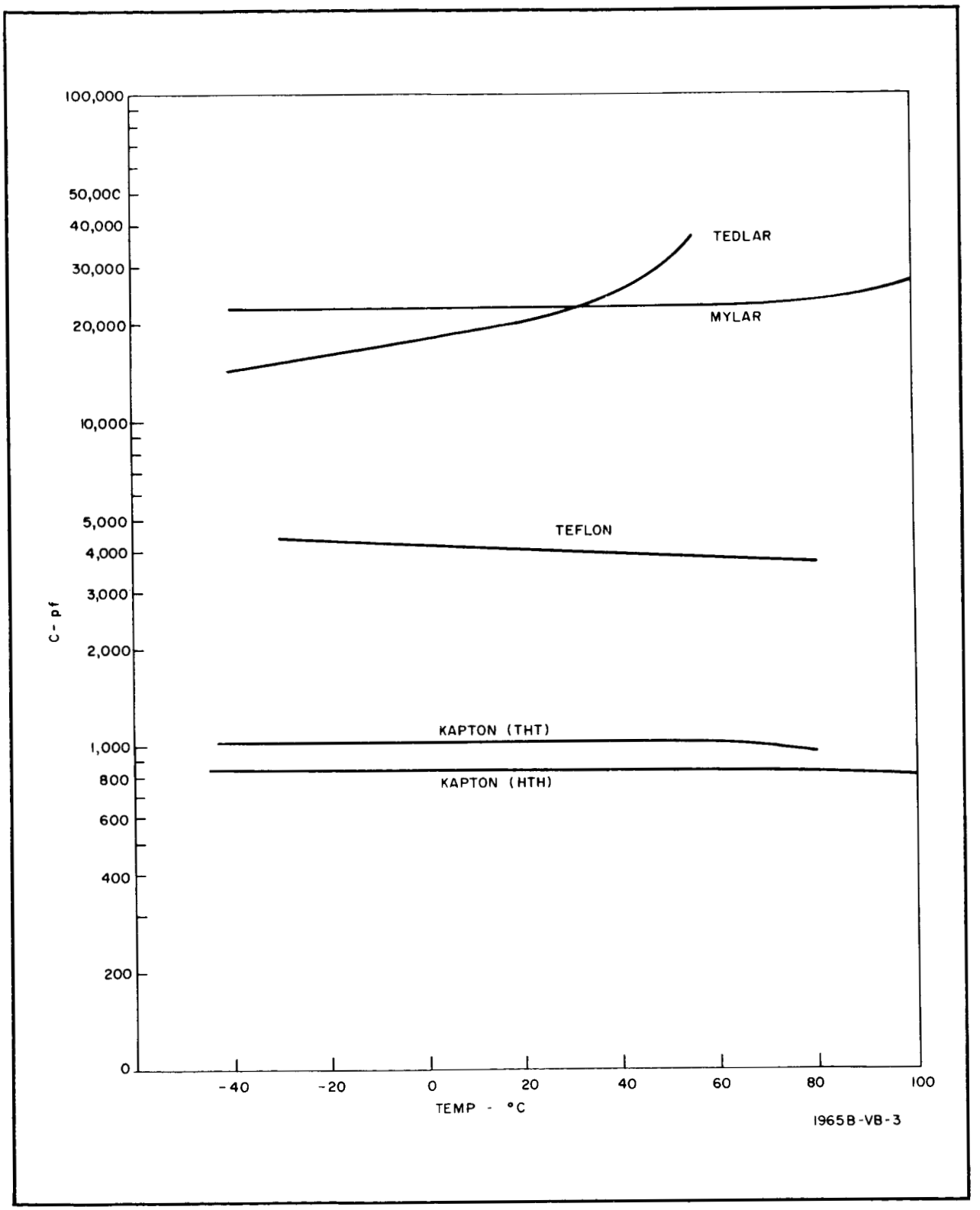

Figure 4-1. Capacitance vs Temperature at 1 cps

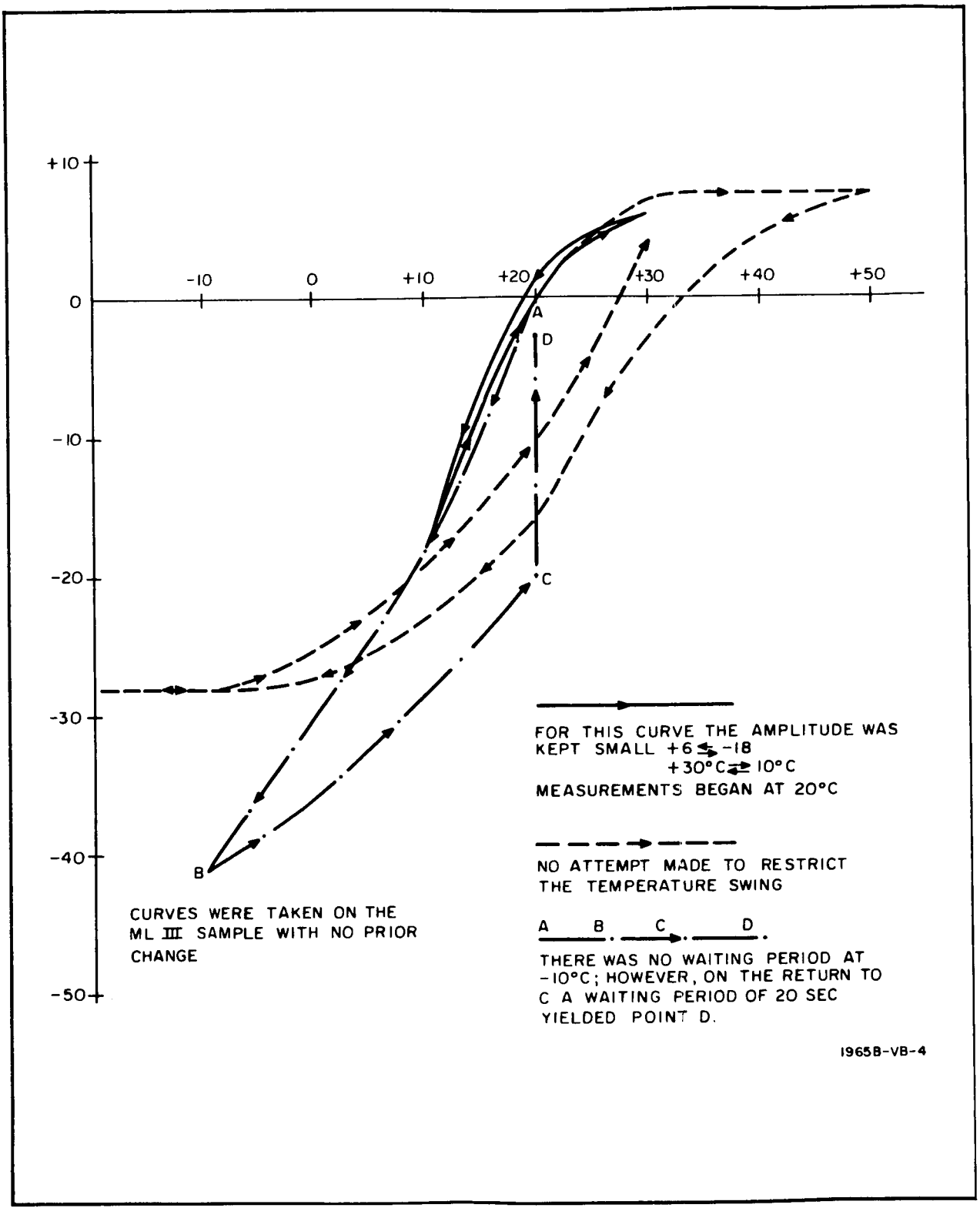

Figure 4-2. Hysteresis Effects in a Thermally Generated Charge

4.4 EFFECT OF SIGN OF CHARGE UPON ENERGY CONVERSION

In those samples which showed the quasi-pyroelectric effect, the ratio of energy conversion was different if the thermoelectrostatic cycle was performed with the ungrounded face of the condensers positive, than if the latter were negative. The choice of sign of charge to utilize in this type of specimen, in order to obtain maximum solar energy conversion, is derived in Appendix A.

4.5 SEARCH FOR, AND ELIMINATION OF POSSIBLE CAUSES OF THE EFFECT

Since the effect produced significant changes in the computed efficiency of energy conversion, an examination was made of possible experimental causes other than true dielectric behavior. A number of possible procedural and apparatus causes, such as the following, were examined and shown not to be causes of the measured effect:

a. Charge transfer from environmental chamber to apparatus. A small amount of transfer was measurable, presumably originating from the control circuit. This was eliminated without any major change of the phenomenon being examined. Also, the samples which did not show the quasi-pyroelectric effect in other environments had not showed it in the environmental chamber.

b. Thermal voltage generation in the sample mounting stand.

c. Leakage from the sun gun. Heating was performed by two other methods. When a commercial hot-filament fan blower was used, large amounts of charge were observed, carried over from the hot filament. When a shielded hot-plate was used, no charges were obtained. Direct test for sun gun leakage showed none. In all cases, only the samples which originally showed the quasi-pyroelectric effect in the environmental chamber exhibited it under any new condition, and all of these did so.

d. Frictional or other charging from the cooling gas (CO_2) which is blown through the environmental chamber to maintain the low temperature. Small voltages were measurable, as also was the case when air and water

vapor were blown through the chamber. However, cooling in the thermal chamber without blown gases (using solid dry ice above the samples) produced the same quasi-pyroelectric effect in the samples which showed it, and none in the others. Direct cooling without CO_2 present showed the same effect.

e. Variac leakage to the electrometer, or circuitry leakage to base.

f. Exposed surface of the lexan. Some samples of the lexan had been sanded on one side. In the first few samples, those with the sanded surface on the outside, and therefore metallized, showed positive effect; those with the smooth side out showed no effect. However, this did not continue.

g. Stray electrical fields. Apparatus was completely shielded, with negligible change in measured results.

Although the above causes were shown not to be responsible for the observed thermal voltage, one environmental factor in these tests was noted; namely, that a small amount of charge leakage (and therefore decreased efficiency) would be caused by deposition of moisture (liquid or solid) on the cooled sample when the door to the chamber was opened, if the temperature were below the dew point. Provision to avoid this was then made; this is not a phenomenon which will take place under space conditions.

4.6 EXPERIMENTAL INVESTIGATION OF THE QUASI-PYROELECTRIC PHENOMENON

4.6.1 Types of Measurements

The following measurements were performed under the environmental conditions specified:

a. Measurement of the voltage generated in the sample as a function of temperature deviation from ambient, together with time constant. Sample uncharged initially. Combined with this were measurements of the dielectric constant of the sample on the low-frequency capacitance bridge.

b. The same, when the electrodes of the sample were charged initially.

c. Both the above, with slow application of charge or of temperature changes, and with rapid, pulsed, charging and/or heating.

d. The above, in different temperature ranges.

4.6.2 Specific Investigative Plan

Recognizing that this phenomenon can contribute to energy conversion efficiency, but is not itself the objective of the contract, a rapid survey type of investigation of two of the better samples was undertaken. The investigative program was as follows:

a. Measurement of capacitance of the sample by bridge, after equilibrium with the environment has been reached in each case, at 50°C and at lower temperatures in the range from -20°C to +10°C.

b. Measurement of the time constant for charge decay at these equilibrium conditions.

c. Measurement of the thermally generated voltage at the upper and the lower limits under the following conditions:

(1) Samples attached to aluminum ring:

(a) No charge on sample initially

(b) Charge applied to sample at 50°C and sample brought to equilibrium. Then change temperature to the lower limit (in a above). For these measurements, sufficient charge applied at the higher temperature to bring the voltage to approximately 5, 10, 15, 25, 50, 100, and 200 volts.

Voltage at lower temperature recorded; measurements repeated so that two measurements taken at each voltage.

(c) Using the same sample in each case as in (b) above, and after the 200 volts measurement, take another set of measurements with sample uncharged; then a set at 200 volts, then a set at 5 volts, then a set at 200 volts, followed by a set at 25 volts.

(d) Repeat (b) and (c) applying the charge at the lower temperature and measuring the voltage at 50°C.

(e) Repeat certain of the measurements with no wait for equilibrium.

(2) Do approximately half of the above measurements for free samples (not attached to aluminum ring).

The results of these measurements are available as raw data; the conclusions which can be drawn from this relatively uninformative raw data are included in this report.

4.7 USE OF VACUUM

4.7.1 Elimination of Effect of Entrapped Air

The most likely hypothesis after the above investigations would seem to be that the air trapped between the two films of the composite is the cause of a portion of the improved energy conversion. This is negated by the facts that:

a. Little change was observed in samples subjected to protracted vacuum before testing.

b. The effect was observed most effectively when the sample was charged at the higher temperature, and discharged at the lower temperature in the cycle. The small decrease in temperature would cause negligible change in the dielectric constant of any entrapped air layer. It would cause a nonnegligible change in the thickness of the air layer. However, this would be a decrease, and therefore the capacitance of the condenser would be greater at the lower temperature. However, this is in direct opposition to the experimentally determined effect; there it was necessary to discharge at the lower temperature in the cycle.

c. The effect was obtained on some homogeneous films.

d. Exposure of the samples to CO_2 for protracted periods of time showed negligible differences in behavior.

4.7.2 Effect of Adsorbed or Absorbed Air

It is unlikely that the small differences in temperature (from 293°K to 273°K, for example) would produce sufficient change in absorbed air in the plastic materials in the experimental time to cause the effects observed.

Adsorbed air could be released or accepted in time periods consonant with the experimental operations. In view of the inertness of the materials being used, and the fact that the major portion of the surface is covered with evaporated metal, it is unlikely that this is a major cause. Since it is not impossible, thermoelectrostatic energy conversion experiments are now beginning to be run in vacuum, after equilibrium conditioning in vacuum. The results will be described in a subsequent report.

4.7.3 Measurements in Vacuum

Two of the better composite samples (mylar-lexan-mylar) were subjected to a thermoelectrostatic cycle in a vacuum of 5×10^{-5} torr, in the apparatus shown in figure 4-3. Capacitance was measured by placing the sample in parallel with a 2000-pf precision fixed condenser outside the vacuum chamber, and charging both to the same initial potential. Upon change of temperature, any change of capacitance of the sample was reflected by a change in voltage across the condenser upon again closing the circuit. Energy conversion was measured with the circuit of figure 2-1 without the branch containing the zener diode, and without the first inductance.

Each sample was allowed to come to equilibrium thermally (several hours), and then the thermoelectrostatic cycle was performed. Heating was by a quartz tube infrared heater (resistance elements inside sealed quartz tube) above the sample. Cooling of the heat source was by radiation, and of the sample by conductive contact of one electrode of the sample to a copper plate to which had been soldered a coil through which liquid nitrogen was pumped. The contact also provided electrical connection to that electrode. Radiation was probably

Figure 4-3. Vacuum, and Metal Evaporation, Equipment

ineffective, since the very low temperature environment characteristic of space was not available. Cooling times were of the order of minutes (up to 7 minutes), instead of the usual 10 to 12 seconds in previous experiments in the atmosphere. On the other hand, because of the use of liquid nitrogen for cooling, the base temperature to which cycling was possible was lower than that previously used.

Various temperature ranges were used for the samples. The results are given in table 4-1. It is evident that the quasi-pyroelectric effect was still present, even though the air film between the halves of the composite material had been removed by the vacuum conditions. The effect was not so great as in the previous environment. This could relate the effect to adsorbed air, or could be due to the somewhat lower temperature range and the amount of time required for cooling which would allow greater leakage and loss of charge through the dielectric material.

Although these samples had shown capacitance change with temperature in air, there appeared to be little if any capacitance change with temperature in vacuum; the demonstrated energy conversion from thermal energy to electrical energy in this case was almost wholly the result of the quasi-pyroelectric effect in the sample. Other materials, however, retain their dependence of dielectric constant upon temperature in the vacuum, and with these, a combined effect, or even a nonextended thermoelectrostatic cycle, is possible.

TABLE 4-1

VACUUM MEASUREMENT RESULTS

Sample	Pressure	Pyroelectric Effect (volts)	Initial Voltage (volts)	Approximate Time For Run (minutes)	$\frac{\Delta E_2}{\Delta E_0}$
1 ML III	5×10^{-5} torr	5	5	10	1.06
2 ML V	5×10^{-5} torr	15	20	20	0.36
3 ML V	5×10^{-5} torr	15	5	15	2.6
4 ML V	5×10^{-5} torr	15	10	20	0.2
5 ML V	16 hours conditioning under vacuum. Measurements under same pressure of 5×10^{-5} torr	10	10	20	<0.1
6 ML V	16 hours conditioning under vacuum. Measurements under same pressure of 5×10^{-5} torr	10	5	20	<0.1
7 ML V	16 hours conditioning under vacuum. Measurements under same pressure of 5×10^{-5} torr	10	5	20	0.78 With the use of more heat
8 ML II	5×10^{-5} torr	11	10	30	<0.1
9 ML II	5×10^{-5} torr	11	5	20	<0.1
10 ML II	5×10^{-5} torr	3	5	20	<0.1

Preliminary experiments. Temperature ranges of cycle not accurately determined. Temperature maximum in test 7 was higher than in tests 4-6. ML II may have shown internal leakage.

5. EXPERIMENTAL DATA

5.1 CAPACITANCE OF MATERIALS AS A FUNCTION OF TEMPERATURE

Examples of the curves obtained for the capacitance of samples fabricated from various materials as a function of temperature have been given in figure 4-1.

5.2 ENERGY CONVERSION BY THE THERMOELECTROSTATIC CYCLE

5.2.1 Data

Relevant data for energy conversion of homogeneous and composite films with thermoelectrostatic cycling are given in table 5-1.

Preliminary results have been communicated to the sponsor directly by letter. The data in table 5-1 are results subsequent to the preliminary data, and taken with added precautions for precision and elimination of possible artifacts.

The energy conversion observed is described by the various columns in table 5-1. The output-input energy ratio is given in the column marked $\Delta E_0/\Delta E_i$. As described above, the energy values are computed from source-condenser energy loss and storage (output) condenser energy gain.

5.2.2 Other Samples

Similar measurements on other samples have yielded output-input energy ratios, R_1, of one or less than one; if energy conversion was obtained, it was lost through leakage or otherwise. These films included various samples as single or composite films of lexan, mylar, copper-clad mylar, Owens-Illinois T-100 resin, aclar, polytherm, vitro film, tedlar, Kapton (1/2 FEP teflon/2 H/1/2 FEP), and (H/FEP teflon/H), Kel-F, polypropylene, teflon (FEP), mica, polyethylene, videne polyester, H-film. The composite films have been laminates of the above with phenolic or vinyl films.

No experimental results were obtained significant to the objective of this work except that mylar single film (vacuum evaporated aluminum electrodes applied here) showed lower leakage than did commercial copper-clad mylar with an aluminum electrode on the other surface; however, the copper-clad mylar showed better capacitance charge with change of temperature.

5.2.3 H-Film/Teflon

Because of the data and considerations reported in the second quarterly report, it was expected that a lamination of H-film with teflon, in which the H-film was on each outside side of the sandwich, would yield good results. Through courtesy of the Film Department of E.I. DuPont de Nemours, Inc., laminated samples of teflon/H-film/teflon, and H-film/teflon/H-film were available for test. These films are designated Kapton in figure 4-1, and it may be seen that for these samples negligible capacitance change with temperature was observed. On the thermoelectrostatic cycling circuit, energy conversion was not observed. The results may have been characteristic of the particular lots of materials used, and not of such a lamination in general, however, in view of the earlier results.

5.3 QUASI-PYROELECTRIC EFFECT

Data with respect to the quasi-pyroelectric effect in the mylar-lexan or mylar-laxan-mylar composite samples are given in table 5-2; the maximum voltage observed is given in each case. It appears from transient observations, that it may be possible to fabricate composite samples with higher maximum voltages than those observed.

Figure 5-1 shows a typical behavior of the sample (copper-clad mylar) if it is grounded at the high temperature near to its onset of conductivity. After this, the thermally generated voltage will not appear until the temperature is raised to a higher temperature than that at which the grounding was performed.

5.4 DIELECTRIC LEAKAGE AS A FUNCTION OF TEMPERATURE

Since dielectric leakage is a direct thief of the energy converted, and since in the work reported in the second quarter it was found that a number of samples which might have had energy conversion possibilities were unsuitable because of leakage, some measurements have been made of this parameter. An

TABLE 5-1

THERMOELECTROSTATIC CIRCUIT ENERGY TEST

Sample	Type	Environment*	Temperature °C		C_0	C_2	V_0 (volts)	V_{f1} (volts)	V_{f2} (volts)	Cycles	$V_0^2 - V_{f1}^2$ (a)	$V_{f2}^2 - V_{01}^2$ (b)	$\Delta E_i = C_{so}/2$ (a) $\times 10^{-3}$	$\Delta E_0 = C_{st}/2$ (b) $\times 10^{-3}$	$\Delta E_0/\Delta E_i$
			T_ℓ	T_h											
MLM #1	3 layer laminate	O	-34		1090	1085	5	3.25	6.75	5	14.5	20.5	7.9	11.2	1.41
		O	-34		1090	1085	10	6.75	13.2	5	54.5	64	29.7	34.7	1.17
		O	-34		1090	1085	15	13.2	17.4	5	61	77	33.3	41.8	1.26
		O	-34		1090	1085	20	17	22	5	111	93	60.5	50.5	0.835
MLM #2	3 layer laminate	O	-20		1090	1085	-10	-5.5	-16	6	69.8	156	38.1	84.6	2.22
		O	-20		1090	1085	-16	-12.5	-20	5	100	144	54.5	78.1	1.43
ML #1	2 layer laminate	O	-30		1090	1085	+20	14	25	5	204	225	111	122	1.1
ML #2	2 layer laminate	O	-7		1090	1085	-20	-11	-30.5	4	279	530	152	288	1.89
ML #3	2 layer laminate	O	-3		1090	1085	-10	-8	-10.2	3	36	4	19.6	2.2	.11
	2 layer laminate	O	-10		1090	1085	-26	-20.5	30	5	256	224	139.6	121.5	.871
	2 layer laminate	C	-10	20	9081	9050	-25	-21	31	3	185	335	843	1515	1.8
ML #4	2 layer laminate	O	-15		1090	1085	+5	3.1	6.6	5	15.4	18.5	8.5	10	1.18
ML #5	2 layer laminate	O	-20		1090	1085	-20	-10.5	-29.5	5	290	468	15.8	25.4	1.60
ML #6	2 layer laminate	O	-20		1090	1085	-10	-5.2	-14.8	5	73	118	39.8	64	1.61
	2 layer laminate	O	-20		1090	1085	-20	-13.8	-25.5	5	210	250	114.5	136	1.19
	2 layer laminate	O	-20		1090	1085	-30	-21.5	-34.5	4	440	285	240	155	0.645
ML #14	2 layer laminate	O	-15		1090	1085	4.6	1.6	7.0	5	18.6	27.9	10.1	15.2	1.5
ML #18	2 layer laminate **	O	-30		1090	1085	-20	-14	-26	5	204	276	111	150	1.35

*O = Oven

*C = Statham Environmental Chamber

V_0 = Voltage on C_0, C_i, and C_2 test

V_{f1} = Voltage of C_0 at the end of the test

V_{f2} = Voltage of C_2 at the end of the test

ML #7 - #13 and ML #15 - #17 were not tested in the energy conversion circuit because of poor preliminary test results

#7, #8, #15, #16, #17 - cemented completely across surface; others were cemented only on the edge.

** = Free unsupported sample.

T_ℓ = Lower temperature.

T_h = Higher temperature (samples were heated by irradiation in the oven environmental chamber; although the general range of higher temperatures was in the range 30-40°C, some deviations because of absorptivity and emissivity uncertainties were present).

TABLE 5-2

THERMALLY GENERATED VOLTAGE MAXIMA

Sample**	$T_{initial}$ °C	T_{final} °C	Apparatus Used ***	Thermal Voltage (volts)
MLM #1	-34	*	O	+5
MLM #2	-20	*	O	+14
ML #1	-30	*	O	-13
ML #2	-7	*	O	-22
ML #3a	-3	*	O	-6
ML #3b	-10	+20	C	-40
ML #4	-15	*	O	+5
ML #5	-20	*	O	+14
ML #6	-20	*	O	-5 to -10
ML #14	-15	*	O	+5
ML #18	-30	*	O	+9
ML #7-13	-20	*	O	No appreciable effect
ML #15-17	-20	*	O	No appreciable effect

* Temperature measurement not precise because of experimental arrangement. Final temperature at least 20°C and possibly up to 40°C.

** M = mylar
L = lexan

*** O = oven
C = Statham Environmental Chamber

example is figure 5-2. Here, voltage was applied to a homogeneous film sample of copper-clad mylar, and the temperature cycled through the ranges indicated on the abscissa. The voltage measured at each temperature, one minute after the temperature was attained, is plotted as the ordinate.

The transient conductivity indicated by the small dip always occurs with a new specimen, and after a considerable rest period. After occurring once, it

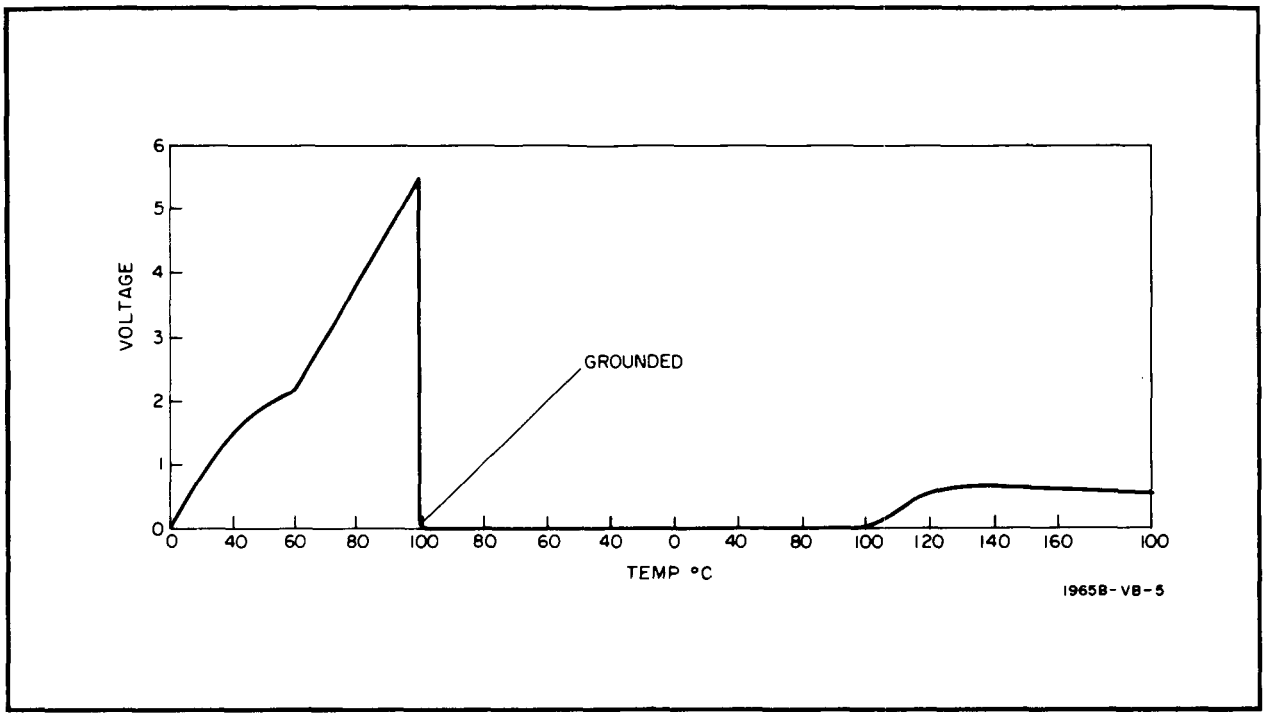

Figure 5-1. Pyroelectric Effect

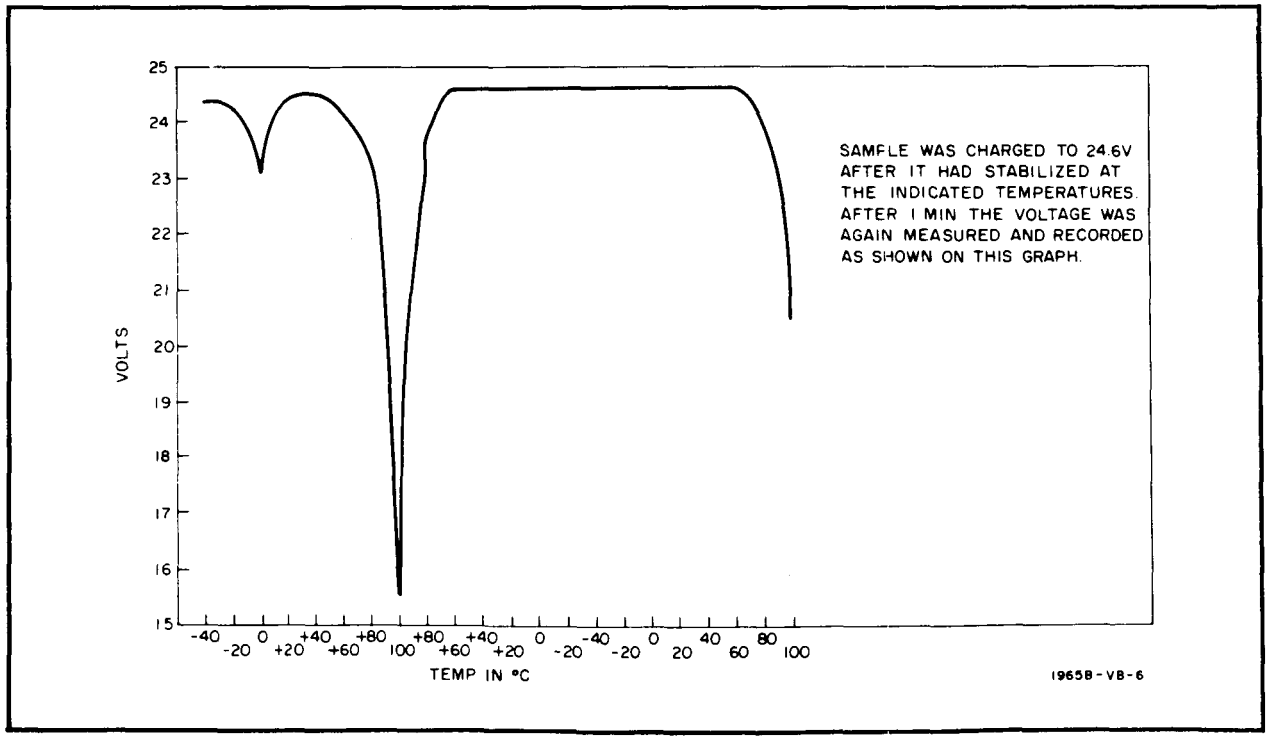

Figure 5-2. Copper-Clad Mylar Leakage

does not repeat in subsequent cycling. The sudden onset of leakage (without electrical harm to the sample) at 100°C is characteristic and repeatable time after time.

5.5 NEW APPARATUS AND CHANGES IN APPARATUS

Both the previously used temperature controlled chamber, and a new chamber shown in figure 5-3 - a Statham temperature controlled test chamber with a working space of 10 by 10 by 6 inches and with 1/4°F precision for chamber walls, and approximately 1/2°C estimated precision for sample temperature - are now being used. The Statham chamber uses CO_2 cooling from tanks, and permits a temperature range from -70°C to 270°C. In the lower range, temperature control is by a pressure reducing valve and a temperature controlled flow switch. Traverse of the whole range in the increasing direction takes 12 minutes, and from 0 to 100°C takes 5 minutes. As mentioned above, the cycle is being speeded up by mounting the sun gun inside the chamber with the sample.

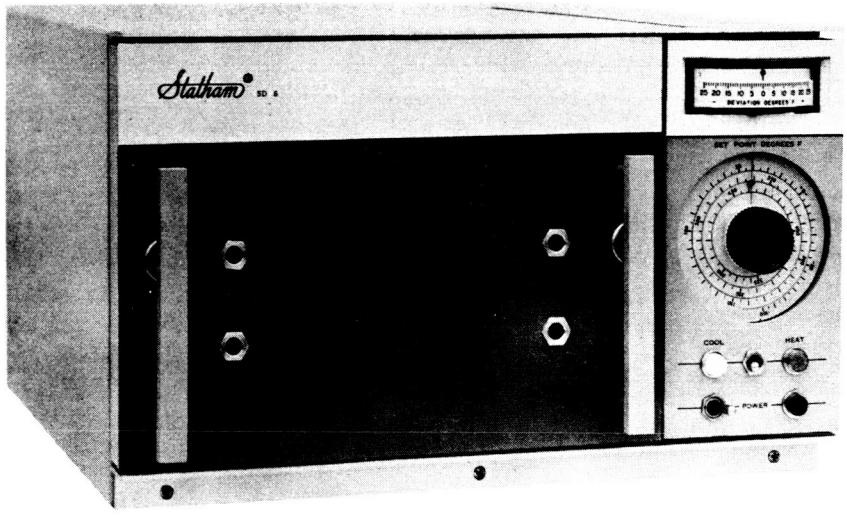

1965B-PF-7

Figure 5-3. Statham Temperature Controlled Test Chamber

A specially designed and built low-frequency capacitance bridge measuring dielectric constant and loss factor on the frequency range of 0.01 to 20 cps is being used. The range of this bridge has been extended from 0 to 1000 pf to the 0 to 10,000 pf range compatible with the larger samples which can be placed in the Statham chamber.

The energy conversion circuit suggested by the sponsor, has been built and is routinely being used for energy conversion measurements of samples. As mentioned above, condenser source and output storage are being used for measurement of energy conversion.

A hexagonal squirrel-cage type mount for six specimens, of size 8 by 8 inches or less, has been built and is now complete with pulleys, belt, and motor. This is on a shaft so that speed reduction gear is possible, and the latter and the bearings have been completed.

5.6 EXPERIMENTAL TECHNIQUES

5.6.1 Fabrication of Samples

A number of sample fabrication techniques have been developed, and used. These include suitable electrode application techniques (vacuum evaporation appears to yield the best results - different results are obtained on the same material when electrodes are applied by different techniques), suitable adhesive bonding of samples to supports, and methods for laminating composite films by pressure, by adhesive, and thermally. Details of the more successful methods have been given in the last two monthly reports.

Both samples supported on aluminum rings, and unsupported samples, have been prepared and measured. In all cases, details have been noted of all fabrication steps, and it is intended to correlate these with the degree of observed thermally generated voltage in the final samples. A number of homogeneous films have been prepared by various techniques, but have shown less effective conversion than do the composite films.

5.6.2 The Use of Lower Temperature Ranges

Lower temperature measurements than in previous reports have been made, both with the Statham chamber and the oven. They introduce the necessity for care that moisture is not deposited in crystalline or liquid form on the surfaces of the sample, and the requirement for periodic checks under constant low temperature environment to ensure that CO_2 adsorption on the electrodes or exposed dielectric surfaces does not affect the results.

However, lower than room temperature ambients appear to be more suitable temperature ranges for the thermoelectrostatic cycle, because the dielectric constant change can be obtained, without excessive electrical leakage.

6. CONCLUSION AND DISCUSSION

6.1 DISCUSSION OF RESULTS

6.1.1 The Practicability of the Thermoelectrostatic Cycle as an Energy Source in Space

During this quarter, unambiguous conversion from solar energy to electrical energy by the thermoelectrostatic cycle has been demonstrated. Energy ratios between output and input energy of over two have been obtained sufficiently often to demonstrate the experimental practicability of the thermoelectrostatic cycle as an energy source.

An effect discovered in certain composite plastic films when properly utilized, makes it possible to increase the energy conversion ratio of the thermoelectrostatic cycle to significantly higher values than are attainable without this effect.

6.1.2 The Quasi-Pyroelectric Effect

Although a number of parameters relating to the quasi-pyroelectric effect have been examined, more detailed examination of other factors is desirable.* The attainable maximum voltage from this effect should be determined, since it is less useful when the working thermoelectrostatic voltages greatly exceed the quasi-pyroelectric additional voltages. The conditions under which the

* Since the objective of the work being performed transcends this particular phenomenon, it has not been investigated for its own sake. If it were to be, it is likely that explanations of the effect would include considerations such as those in: "Dielectric Behavior of Nonrigid Molecules: II. Intramolecular Interactions and Dielectric Relaxation," R. K. Fong, RCA Review 25, 752 (1964). "Dielectric Relaxation as a Chemical Rate Process," W. Kauzmann, Rev. Mod. Phys. 14, 12, (1942). "Electromechanical Hysteresis Measurements: A New Tool for Investigation of the Properties of Plastics," E. L. Kern and S. M. Skinner. J. App. Polymer Sci. 22, 404 (1962).

quasi-pyroelectric voltage is obtained need definitizing: in a few samples made by nearly the same fabricational technique from apparently identical materials in a different batch, the effect was not observed. Also, it should be determined whether the effect is an inherent property of the material which will persist even after prolonged cycling and prolonged exposure to space environment.

6.1.3 Additional Plastic Materials

A large number of plastics have been examined during the work of the last two quarters, and initial parameters permitting choice of those most favorable have been determined. Not all available plastics have yet been examined. Others should be examined under a rough survey program, and favorable ones examined more in detail. Also, a considerable number of other possibilities for composite films, by lamination or otherwise, exists, in which the parameters already determined can be used to provide choice of the desirable combinations and avoidance of unsuitable ones.

6.2 FUTURE WORK

It is intended during the next quarter to continue the direct examination of the thermoelectrostatic cycle with the materials which have shown the most promise, to examine some new materials, and to perform initial vacuum measurements on more samples. Other work which will be chosen will be determined in conference with the sponsor, from the various desirable possibilities suggesting themselves as the result of the work performed to date. These include such objectives as design of a prototype thermoelectrostatic generator, optimization of the materials and cycle, improvement of experimental methods, more extensive and thorough examination of particular portions of the experimental work, experiments at the maximum attainable working voltages (including consideration of dielectric breakdown), or other subject matter contributing to the sponsor's objectives.

7. REFERENCES

1. B. H. Beam, "An Exploratory Study of Thermoelectrostatic Power Generation for Space Flight Applications," NASA TN D-336, October 1960.
2. B. H. Beam, "Analysis of Solar Energy Conversion Using Thin Dielectric Films," NASA TM X-50, 136, July 1963.
3. Proposal, "Thin Dielectric Films for Energy Conversion," Westinghouse Electric Corporation, Neg. No. AAN-32650, February 1964.
4. B. H. Beam, J. F. Fry and L. D. Russell, "Experiments on Radiant Energy Conversion Using Thin Dielectric Films," Presented at the AIAA Power Systems Conference in Philadelphia, 3 September 1964.
5. "Investigation of Thin Dielectric Films for Energy Conversion," Quarterly Report No. 1, 15 September 1964, to Ames Research Center, NASA, by Westinghouse Electric Corporation.
6. "Investigation of Thin Dielectric Films for Energy Conversion," Quarterly Report No. 2, 15 December 1964, to Ames Research Center, NASA, by Westinghouse Electric Corporation.

APPENDIX A

INCREASE OF ENERGY CONVERSION EFFICIENCY BY USE OF THERMALLY GENERATED VOLTAGE IN PLASTIC MATERIALS

A. 1 COMPLEMENTATION OF THE THERMOELECTROSTATIC ENERGY CONVERSION CYCLE BY THE THERMALLY GENERATED VOLTAGE IN PLASTIC MATERIALS

In the first quarterly report on this contract, it was shown that composite materials, including ferroelectric substances compounded with plastic binders, should exhibit a considerable energy conversion efficiency. In discussion with the sponsor, it was decided to continue work with plastic films, primarily because of their thinness, their light weight, and the high resistivity achievable as compared with ferroelectrics. This has turned out to be a wise decision. The expected advantages have been confirmed. In addition to these advantages, the thermally generated voltage in the composite plastic samples (described in paragraph 4 of the text) permits additional energy conversion efficiency over that which would be expected from a simple material. This additional energy conversion efficiency in the extended thermoelectrostatic cycle is derived below, and a numerical example is computed using experimental values.

The thermally generated voltage is apparently not explainable by air or other gas entrapment in the sample, but appears to be a fundamental property of the plastic itself. If this is confirmed, and if sufficiently high values of the voltage can be obtained, the effect can be utilized to achieve a high ratio of energy conversion in a suitably designed converter in a space vehicle. It should be noted, however, that a number of additional confirmatory, and optimization experiments are still necessary to assure that stability and reproducibility are possible throughout the period of a space voyage, or a 6-month succession of satellite orbitings.

A.2 THE THERMALLY GENERATED VOLTAGE

Although the thermally generated voltage shows hysteresis effects throughout a considerable portion of its range, it is nearly linear with temperature. Under appropriate design conditions the hysteresis loop is quite thin, and therefore a direct linear dependence upon temperature describes the phenomenon quite well. Since the voltage disappears with time (with a time constant considerably longer than the duration of a single thermoelectrostatic cycle), its value at the commencement of cycling is zero. The generated voltage is therefore directly proportional to the temperature excursion from ambient; i.e.,

$$\overline{V}(T) = k\,(T - T_a) \tag{A-1}$$

where T_a is the initial temperature of the sample, achieved by immersion of the sample in an ambient temperature environment for periods exceeding, say, five time constants of the thermal voltage generation transient.

This voltage will add algebraically to the voltage put on the sample by the charge imparted to it in the thermoelectrostatic cycle. Thus, if a charge Q is placed on the sample, whose capacitance as a function of T is C(T), the total voltage across the sample will be

$$V = \frac{Q}{C(T)} + \overline{V}(T) = \frac{Q}{C(T)} + k(T - T_a) \tag{A-2}$$

Utilizing the linear capacitance relationship of reference 2:

$$\begin{aligned} V &= \frac{Q}{C_0}\,\frac{1}{1 + \beta\,(T - T_a)} + k\,(T - T_a) \\ &= \frac{Q}{C_0}\,\Big[1 - \beta\,(T - T_a)\Big] + k\,(T - T_a) \\ &= \frac{Q}{C_0} - \left(\frac{Q\beta}{C_0} - k\right)(T - T_a) \end{aligned} \tag{A-3}$$

Since the sign of charge placed on the condenser can be chosen, it is possible to make the terms in the first parenthesis additive.

A. 3 THE EXTENDED THERMOELECTROSTATIC CYCLE

In the derivation below, it is assumed that, because of the thermally generated voltage, an increase of temperature puts a positive voltage on the reference electrode; therefore, k is positive. This involves no loss of generality.

In order that the maximum energy conversion be obtained, a definite relation of polarity of charging to the dependence of the dielectric constant on temperature must be chosen. As is well known, if the dielectric constant decreases as temperature increases, the thermoelectrostatic cycle requires that charging be performed at the lower temperature, and discharging be done at the higher temperature. In order that the thermally generated voltage supplement the energy conversion favorably, the sign of charge must be such that at charging the electrode is (thermally) charged opposite to the charge placed upon it from condenser C_0. Then during the temperature change, decrease of dielectric constant raises the working condenser voltage, and simultaneously the change in temperature creates an added voltage of the same sign, so that at discharge, the working thermoelectrostatic condenser is characterized by a higher temperature than if the second effect were not present. The thermally generated voltage created by the temperature should be in the same direction as that of the originally imparted voltage from charging. The sign of charge placed on the condenser is therefore governed by the table below:

β	$T_{chg} \gtrless T_{dischg}$	k	Voltage Applied to Reference Electrode
-	<	+	+
-	<	-	-
+	>	+	-
+	>	-	+

As an example, if the temperature of charging is 0°C, the temperature of discharge is 20°C, and the ambient temperature of the sample is 0°C, let the dielectric produce a positive voltage of 12 volts with a 10°C temperature difference on the reference electrode of the condenser as the temperature increases. The voltage on the sample before charging is:

$$\overline{V}\,(0°C) = 0$$

Connect sample to 100-volt supply, reference electrode positive.

$$Q_{\text{from supply}} = C(0°C) \cdot 100$$

Raise the temperature to 20°C. Assume that the capacitance at the higher temperature is 0.4 that at the lower temperature. Then

$$V(20°C) = \frac{100}{0.4} + 24 = 274 \text{ volts} \qquad \text{(A-4)}$$

To achieve the same higher voltage,* the dielectric constant would have had to be reduced to 0.365 of its previous value. The energy conversion ratio with the extended thermoelectrostatic cycle will be 2.74 instead of 2.5, as with the simple thermoelectrostatic cycle.

* It should be noted that some samples appear to yield a higher voltage than that computed in this manner. If the capacitance change measured on the capacitance bridge is used to compute the voltage expected from the initial charge placed on the sample, and to it is added the independently measured thermally generated voltage, the thus computed voltage at the second temperature is less than that measured experimentally. Any nonlinearity thus observed at a charged sample as compared to an uncharged sample appears to enhance the energy conversion.

APPENDIX B

ENERGY TRANSFER AND BUILDUP IN THE THERMOELECTROSTATIC ENERGY CONVERSION CIRCUIT OF B. H. BEAM WITH CONDENSER SOURCE AND CONDENSER OUTPUT STORAGE

B. 1 ADVANTAGES AND DISADVANTAGE OF CONDENSER SOURCE AND LOAD

Precise measurement of energy transfer is necessary; this is a very different problem experimentally from measurement of charge or voltage. Use of precision condensers as the source and storage for the load, in conjunction with the thermoelectrostatic circuit, has the important advantage that the output energy delivered and the energy taken from the source can be computed accurately and without question from the capacitances and voltages of the condensers.

So far as the source, at least, is concerned, this is also a realistic representation of the use of the cycle in space application; because of the prohibitive weight of battery sources, it is likely that the source for charging the working thermoelectrostatic element will be a condenser (reference 2). A condenser is also a useful storage device until the apparatus in the space vehicle uses the energy; such storage of energy has been included in the circuit diagram of figure B-1, which differs only by rearrangement from that furnished by the sponsor.

Condenser sources, if used alone, suffer from the disadvantage of energy loss accompanying charge transfer. As shown in reference 2, and as computed in Appendix C hereto, most of this energy loss can be overcome by adding an inductance and diode in the energy transfer circuit. The inductance-diode combinations shown in figure B-1 accomplish this for the successive steps in the cycle. As mentioned elsewhere, the use or nonuse of such an inductance in a power source for a space vehicle must be weighed

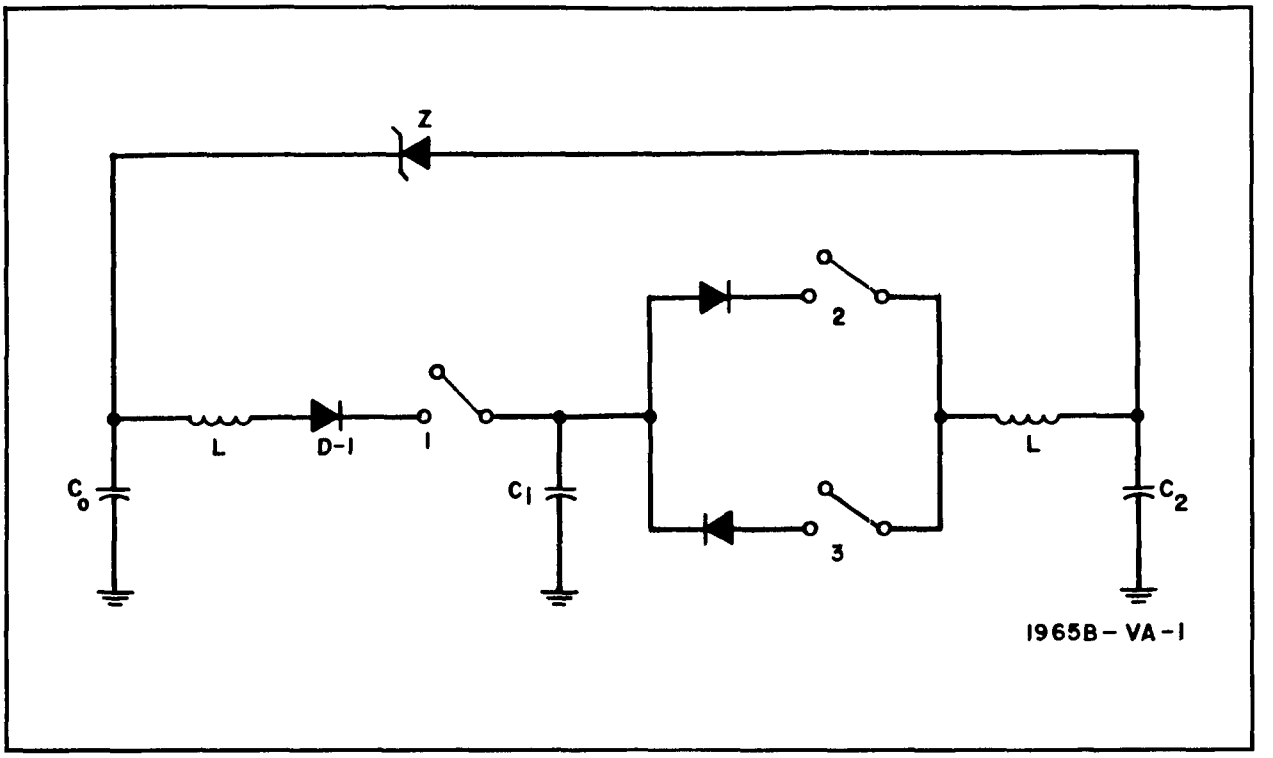

Figure B-1. Thermoelectrostatic Energy Conversion Circuitry

against the weight penalty, but if it can be used, the conversion efficiency is increased.

In the experiments described in this report, no inductance was included in the branch of the circuit between C_0 and C_i. Therefore, the energy values given could be improved by the removable energy loss in the successive charge transfers from C_0 to C_i, yielding an even greater ratio of output energy to input energy than reported.

B.2 ENERGY CONVERSION IN THE THERMOELECTROSTATIC CYCLE, WITH INDUCTANCES AND DIODES

Assume that the inductor and diode are used in each branch of figure B-1. * Let the initial charge on C_0 be q_{00}, that on C_i be q_{i0}, and the charges after

* If an inductance is omitted, the relations derived here are altered by substitution of equation C-8, and C-11, and C-12, for C-6 and C-9 for the transfers of charge and energy in the step involving that branch.

the first switch closing be designated q_{01} and q_{i1}.* Successive switch closings or temperature change steps will cause changes in charges which will be designated by successively increasing second subscripts; i.e., q_{i2}, etc.

Step 1. Charging of C_i from C_0

Using the relationships developed in Appendix C and letting E stand for energy,

$$\left.\begin{aligned} q_{01} &= \left[q_{00}\,(C_0 - C_i) + 2q_{i0}C_0\right] \Big/ (C_0 + C_i) \\ q_{i1} &= \left[q_{i0}\,(C_i - C_0) + 2q_{00}C_i\right] \Big/ (C_0 + C_i) \\ q_{i1} &= q_{20} \\ -\Delta E_{01} &= 2\,(q_{00} + q_{i0})\,(C_i q_{00} - C_0 q_{i0}) \Big/ (C_0 + C_i)^2 = \Delta E_{i1} \end{aligned}\right\} \qquad \text{(B-1)}$$

Step 2. Change of Dielectric Constant by Change of Temperature

Because of temperature change, the dielectric constant ϵ becomes ϵ_a, where $a > 1$. Therefore:

$$C_i \rightarrow C_i/a;\ V_{i2} \rightarrow aV_{i1};\ q_{02} = q_{01},\ q_{i2} = q_{i1},\ q_{22} = q_{21} \qquad \text{(B-2)}$$

Step 3. Charging of C_2 From C_i/a

Again using the relationships in Appendix C with appropriate subscripts,

$$\left.\begin{aligned} q_{03} &= q_{02} \\ q_{i3} &= \left[q_{i2}\,(\frac{C_i}{a} - C_2) + 2q_{22}\,\frac{C_i}{a}\right] \Big/ (C_2 + \frac{C_i}{a}) \\ q_{23} &= \left[q_{22}\,(C_2 - \frac{C_i}{a}) + 2q_{i2}C_2\right] \Big/ (C_2 + \frac{C_i}{a}) \\ -\Delta E_{i3} &= 2\,(q_{i2} + q_{22})\,(C_2 q_{i2} - \frac{C_i}{a} q_{22}) \Big/ (C_2 + \frac{C_i}{a})^2 \end{aligned}\right\} \qquad \text{(B-3)}$$

* As is evident, the first subscript refers to the condenser which has that charge or has gained or lost that energy after the step.

Step 4. Change of Dielectric Constant by Temperature Change

$$\frac{C_i}{a} \rightarrow C_{i1};\ V_{i4} \rightarrow \frac{V_{i3}}{a};\ q_{04} = q_{03},\ q_{i4} = q_{i3},\ q_{24} = q_{23} \tag{B-4}$$

Step 5. Charging of C_i From C_0

At this point, charge taken from C_0 has been delivered to C_2 with increased energy content. The dielectric constant change in step 4 decreases the voltage on C_i to below that of C_0 after its loss of charge. By closing switch 1, additional charge is taken from C_0.

$$\left.\begin{aligned} q_{05} &= \left[q_{04}(C_0 - C_{i1}) + 2q_{i4}C_0\right] \Big/ (C_0 + C_i) \\ q_{i5} &= \left[q_{i4}(C_i - C_0) + 2q_{04}C_i\right] \Big/ C_0 + C_i \\ q_{25} &= q_{24} \\ -\Delta E_{05} &= 2(q_{04} + q_{i4})(C_i q_{04} - C_0 q_{i4}) \Big/ (C_0 + C_i)^2 = \Delta E_{i5} \end{aligned}\right\} \tag{B-5}$$

Step 6. Recharging of C_0 Through the Zener Diode

Step 5 has reduced V_0 to q_{05}/C_0. When this is less than $V_{25} - Z$, charge will flow from C_2 to C_0 through the Zener diode. With the condition that $V_{06} = V_{26} - Z$, the following relations can be shown to be valid:

$$\left.\begin{aligned} q_{06} &= \left[C_0(q_{25} + q_{05} - CZ)\right] \Big/ C_2 + C_0 \\ q_{i6} &= q_{i5} \\ q_{26} &= C_2(q_{25} + q_{05} + CZ) \Big/ C_2 + C_0 \\ -\Delta E_{26} &= \left[(C_2 + C_0)^2 q_{25}^2 - C_2^2 (q_{25} + q_{05} - C_0 Z)^2\right] \Big/ 2C_2 (C_2 + C_0)^2 \\ \Delta E_{06} &= \left[C_0^2 (q_{25} + q_{05} - C_2 Z)^2 - (C_2 + C_0)^2 q_{05}^2\right] \Big/ 2C_0 (C_2 + C_0)^2 \end{aligned}\right\} \tag{B-6}$$

Step 7. Charging of C_i by Connection to C_2

C_2 is still at a higher voltage than is C_i after step 5. Therefore by closing switch 3, charge is brought from C_2 to C_i to use as the "fluid" into

which additional solar energy is to be "pumped." After this charge transfer has taken place,

$$\left.\begin{aligned} q_{07} &= q_{06} \\ q_{i7} &= \left[q_{i6}\,(C_i - C_2) + 2q_{26}C_i\right] \Big/ C_i + C_2 \\ q_{27} &= \left[q_{26}\,(C_2 - C_i) + 2q_{i6}C_2\right] \Big/ C_i + C_2 \\ -\Delta E_{27} &= 2\,(q_{i6} + q_{26})\,(C_2 q_{i6} - C_i q_{26}) \Big/ (C_i + C_2)^2 \end{aligned}\right\} \qquad \text{(B-7)}$$

Step 8. Change of Dielectric Constant by Change of Temperature

$$C_i \rightarrow \frac{C_i}{a}\,;\; q_{08} = q_{07};\; q_{i8} = q_{i7};\; q_{28} = q_{27} \qquad \text{(B-8)}$$

Step 9. Charging of C_2 by Connection With C_i

By closing switch 2, C_2 and C_i are connected through the inductor and diode. Then,

$$\begin{aligned} q_{09} &= q_{08} \\ q_{i9} &= \left[q_{i8}\,(\frac{C_i}{a} - C_2) + 2q_{28}\frac{C_i}{a}\right] \Big/ (\frac{C_i}{a} + C_2) \\ q_{29} &= \left[q_{28}\,(C_2 - \frac{C_i}{a}) + 2q_{i8}C_2\right] \Big/ (\frac{C_i}{a} + C_2) \\ -\Delta E_{i9} &= 2\,(q_{i8} + q_{28})\,(C_2 q_{i8} - \frac{C_i}{a}\,q_{28}) \Big/ (\frac{C_i}{a} + C_2) = \Delta E_{29} \end{aligned} \qquad \text{(B-9)}$$

Succeeding Steps.

The steps from step 4 to step 9 inclusive constitute the cycle which is repeated throughout the use of the energy conversion system. In each cycle, energy transfer is accomplished. When the equilibrium state has been reached, and no energy is being withdrawn,

$$\begin{aligned} V_0 &\geq V_2 - Z \\ q_{04} &\geq C_0 V_2 - C_0 Z = \frac{C_2}{C_0}\,q_{02} - C_0 Z \end{aligned} \qquad \text{(B-10)}$$

Also, since, at steady state, the condition at the beginning of each cycle is the same;

$$\left.\begin{aligned} q_{09} &= q_{03} = q_{04};\ q_{i9} = q_{i3} = q_{i4} \\ q_{29} &= q_{23} = q_{24} \end{aligned}\right\} \qquad \text{(B-11)}$$

B.3 ENERGY CONVERSION IN THE STEADY STATE THERMOELECTROSTATIC CYCLING

B.3.1 The Steady State

By tracing the relations of B-11 through the various steps from q_{09} to q_{04}, etc, three relationships are obtained for the three quantities:

$$Q_0 = q_{09},\ Q_i = q_{i9},\ Q_2 = q_{29} \qquad \text{(B-12)}$$

The ratio, R_1, between output energy and input energy must consider that in the steady state phase of the cycle energy was abstracted from C_0 in step 5 and returned to it in step 6. Also, energy was delivered to C_2 in step 9, but some of this energy was abstracted in steps 6 and 7. Therefore,

$$R_1 = \frac{\Delta E_{29} - |-\Delta E_{26}| - |-\Delta E_{27}|}{|-\Delta E_{05}| - |\Delta E_{06}|} \qquad \text{(B-13)}$$

The final computation of the energy ratio, along with the working quantities in the condensers, is lengthy and will be reserved for the next quarterly report. In the experiments performed here, the condenser C_2 was of the same capacitance as the condenser C_0. Letting the value of both capacitances be C, and the capacitance C_i be gC, the results in paragraphs B.3.2 and B.3.3 are obtained.

B.3.2 Charge Contents in the Steady State

Under these conditions, the charges Q are determined by the equations:

$$\sum_{j=1}^{3} (\alpha_{ij} x_j + \beta_i) = 0$$

$$i = 1, 2, 3. \qquad \text{(B-14)}$$

where

$$x_1 = Q_0/CZ,\ x_2 = Q_i/CZ,\ x_3 = Q_2/CZ$$

Here

$$\left.\begin{aligned}
\beta_1 &= (1+g)\left[1+g+2g^2+\frac{1}{a}\,(-g+g^2)\right] \\
\beta_2 &= g\,(1+g)\left[\frac{1}{a}\,(2-g)-1\right] \\
\beta_3 &= 1 \\
a_{11} &= 1+3g^2,\ a_{12} = 2\,(g^2+1),\ a_{13} = (1+g)\,2g\,(g-\frac{1}{a}) \\
a_{21} &= \frac{g}{a}\,(2+3g+3g^2)-g^2+1,\ a_{22} = -2\,(1+g+g^2+\frac{g^2}{a}), \\
a_{23} &= g\,(1+g)\left[\frac{1}{a}\,(2-g)-1\right] \\
a_{31} &= 1+3g,\ a_{32} = -2,\ a_{33} = -1
\end{aligned}\right\} \qquad \text{(B-15)}$$

The charges derived by solving these equations are those at the beginning of step 4. For determination of the maximum voltages to which any dielectric is subjected, account should be taken of the succeeding values as determined by the cycle equations.

B.3.3 Energy Conversion Ratio

From equation B-13, there can be derived:

$$\left.\begin{aligned}
R_1 &= \frac{16A-B}{16C-D}\,, \\
&\text{where} \\
A &= (q_{i8}+q_{28})\,(q_{i8}-\frac{g}{a}\,q_{28})-(q_{i6}+q_{26})\,(q_{i6}-gq_{26}) \\
B &= (\frac{g}{a}+1)^2\left[4q_{25}^2-(q_{25}+q_{05}-CZ)^2\right] \\
C &= (q_{04}+q_{i4})\,(gq_{04}-q_{i4}) \\
D &= (1+g)^2\left[(q_{25}+q_{05}-CZ)^2-4q_{05}^2\right]
\end{aligned}\right\} \qquad \text{(B-16)}$$

B.3.4 Numerical Example

If the capacitances of all three condensers are the same, g = 1. Under these circumstances, solution of the equations yields:

$$Q_0 = \frac{a^2 - 15\,a + 3\,CZ}{3\,a^2 - 15\,a + 4}$$

$$Q_i = \frac{2\,a\,(5\,a - 9)\,CZ}{3\,a^2 - 15\,a + 4}$$

$$Q_2 = \frac{a\,(-15\,a + 7)\,CZ}{3\,a^2 - 15\,a + 4}$$

For a ratio of maximum to minimum dielectric constant of $a = 4$, the energy conversion ratio of 2.08 is obtained. Better values, and better ratios of energy conversion ratio to a can be obtained.

B.4 THE THERMOELECTROSTATIC CYCLE IN A WORKING POWER SOURCE

The equations developed permit choice of cycle parameters so that suitable energy conversion ratios can be obtained. They also yield the charges and therefore the voltages which are found on the condensers at various stages of the cycle; as a result, they permit design of the cycle so that dielectric breakdown limits of the condensers are not exceeded.

APPENDIX C

ENERGY TRANSFER IN A SINGLE STEP IN THE THERMOELECTRIC CYCLE, WITH CONSIDERATION OF INDUCTANCE

C.1 TRANSIENTS IN THE CHARGE AND ENERGY TRANSFER

The circuit representing any single switch-closing step in the Beam circuit (figure 2-1 of the text) is that of figure C-1. Here the diode is assumed to be a perfect switch, with infinite resistance in the reverse direction and negligible resistance in the forward direction. In the initial charging, L is zero or finite, depending on whether it is decided to omit or include an inductance between C_0 and C_i in figure 2-1 of the text. During the cycling, the inductance L is large. The formulation and boundary conditions are:

$$-L\frac{dI}{dt} + \frac{q_1}{C_1} - \frac{q_2}{C_2} - IR = 0 \qquad \text{(C-1)}$$

$$q_1 = q_{10} - \int_0^t I\,dt$$
$$q_2 = q_{20} + \int_0^t I\,dt \qquad \text{(C-2)}$$

at

$$t = 0:\ I = 0;\ L\frac{dI}{dr} = \frac{q_{10}}{C_1} - \frac{q_{20}}{C_2} \qquad \text{(C-3)}$$

The usual oscillatory, nonoscillatory, and critically damped solutions are obtained. The critically damped solution is the limit of the other two and does not need special consideration. We use the abbreviation C for $\left[C_1 C_2/(C_1 + C_2)\right]$.

In the nonoscillatory solution, the charge transferred between condensers is computed by integrating the integral in equation C-2 between 0 and infinity.

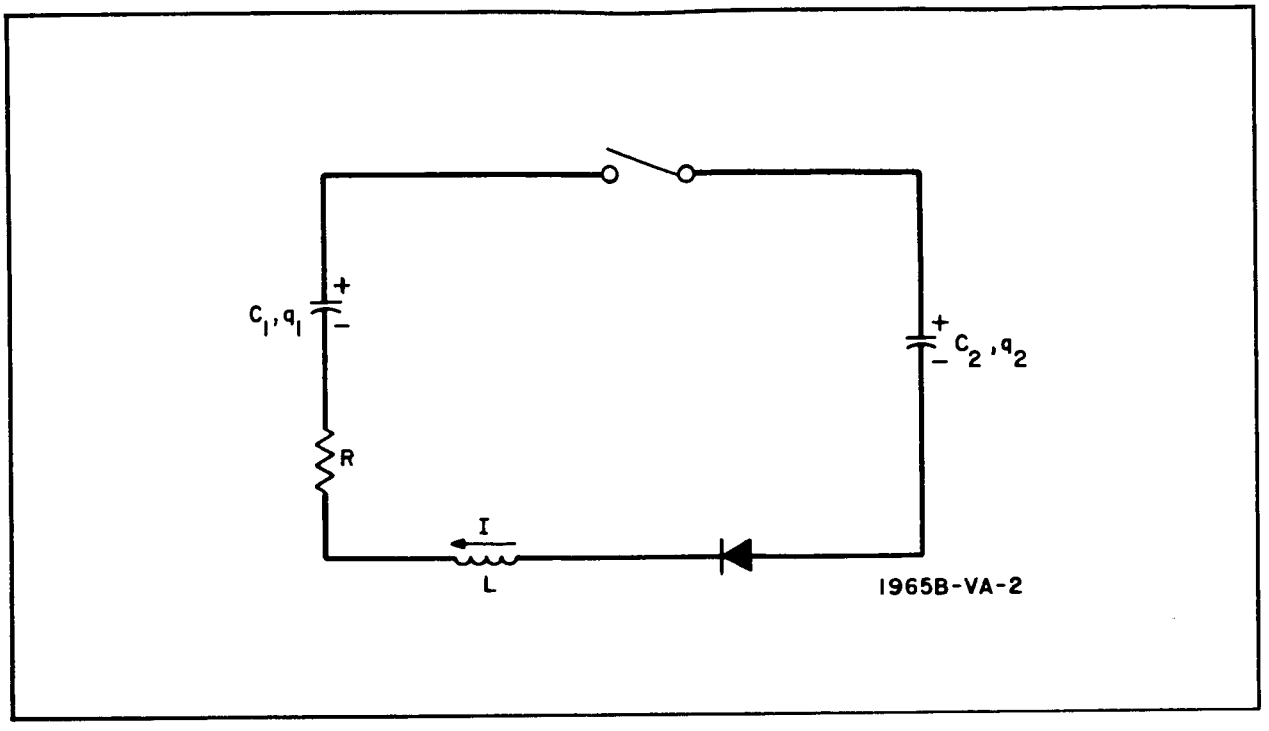

Figure C-1. Circuit for Single Switch - Closing Step

In the oscillatory solution, idealized, the charging of C_2 by C_1 continues throughout the first half-cycle of the current flow oscillation, but because of the diode the current flow is cut off when the current would normally reverse. Therefore, the charge transferred is obtained by integrating between t = 0 and $t = \pi/\omega$.

Energy transfer is computed from the final and initial charges in the two condensers after current flow has ceased.

C.2 CHARGE TRANSFER IN THE OSCILLATORY CASE WITH DIODE CUT OFF

Here,

$$\frac{1}{LC} > \frac{R^2}{4L^2}.$$

Solution of equations C-1 to C-3 yields:

$$I = \left(\frac{q_{10}}{C_1} - \frac{q_{20}}{C_2}\right) (L\omega)^{-1} \; e^{-bt} \sin \omega t \qquad \text{(C-4)}$$

$$b = R/2L; \; \omega^2 = (LC)^{-1} - (R^2/4L^2)$$

$$\left.\begin{aligned} \int_0^{\pi} I dt &= \left(\frac{q_{10}}{C_1} - \frac{q_{20}}{C_2}\right)\left[1 + \exp\left\{-\frac{\pi}{2}\left(\frac{4L}{R^2C} - 1\right)^{-1/2}\right\}\right] \\ \text{and if } (L/R^2C) &>> 1, \\ \int_0^{\pi} I dt &= \left(\frac{q_{10}}{C_1} - \frac{q_{20}}{C_2}\right)\left[2 - \frac{\pi R}{4}\sqrt{\frac{C}{L}}\right] \end{aligned}\right\} \qquad \text{(C-5)}$$

If appreciable resistance (as compared with the inductance) exists in the circuit, the charge transfer is decreased. Assuming that the resistance-inductance ratio is negligible, the final charges on the two condensers are:

$$\left.\begin{aligned} q_{1f} &= \left[q_{10}(C_1 - C_2) + 2\, q_{20}\, C_1\right] / (C_1 + C_2) \\ q_{2f} &= \left[2\, q_{10}\, C_2 + q_{20}(C_2 - C_1\right] / (C_1 + C_2) \end{aligned}\right\} \qquad \text{(C-6)}$$

C.3 CHARGE TRANSFER IN THE NONOSCILLATORY CASE

If the resistance is appreciable, so that

$$\left(\frac{R^2}{4L^2} > \frac{1}{LC}\right),$$

the solution is:

$$\left.\begin{aligned} I &= \left(\frac{q_{10}}{C_1} - \frac{q_{20}}{C_2}\right) \frac{1}{L(a_2 - a_1)} \left[\exp(-a_1 t) - \exp(-a_2 t)\right] \\ \text{where} \\ a_1, a_2 &= \frac{R}{2L} \pm \left(\frac{R^2}{4L^2} - \frac{1}{LC}\right)^{1/2} \\ \int_0^{\infty} I dt &= \frac{q_{10}\, C_2}{C_1 + C_2} - \frac{q_{20}\, C_1}{C_1 + C_2} \end{aligned}\right\} \qquad \text{(C-7)}$$

so that the final charges on the two condensers are:

$$\left.\begin{aligned} q_{1f} &= C_1 (q_{10} + q_{20}) / (C_1 + C_2) \\ q_{2f} &= C_2 (q_{10} + q_{20}) / (C_1 + C_2) \end{aligned}\right\} \qquad (C\text{-}8)$$

C.4 COMPARISON OF THE DIODE-LIMITED OSCILLATORY CASE WITH THE NONOSCILLATORY CASE

In both cases, it is evident that total charge is preserved. In the first case, sufficient charge has been transferred so that a reverse voltage exists which would initiate further oscillation, if the diode were not present to prevent this. In the second case, the final voltages on the two condensers oppose each other and are equal in magnitude.

C.5 ENERGY TRANSFER IN THE TWO CASES

The computation of the total stored energy in both condensers shows the following.

C.5.1 Oscillatory

In the oscillatory case, the sum total energy is the same as it was initially. The energy has been transferred without loss. The amount of energy transferred from C_1 to C_2 is:

$$\Delta E = 2 (q_{10} + q_{20}) (C_2 q_{10} - C_1 q_{20}) / (C_1 + C_2)^2 . \qquad (C\text{-}9)$$

C.5.2 Nonoscillatory

In the nonoscillatory case, the sum total energy has been decreased by an amount:

$$\text{Energy loss to heat} = (C_2 q_{10} - C_1 q_{20})^2 / 2C_1 C_2 (C_1 + C_2) \qquad (C\text{-}10)$$

The energy lost by the condenser, C_1, is

$$-\Delta E_1 = \frac{(C_2 q_{10} - C_1 q_{20}) (C_2 q_{10} + C_1 q_{20} + 2 C_1 q_{10})}{2 C_1 (C_1 + C_2)^2} \qquad (C\text{-}11)$$

The energy gain of the condenser C_2 is

$$\Delta E_2 = \frac{(C_2 q_{10} - C_1 q_{20}) (C_2 q_{10} + C_1 q_{20} + 2 C_2 q_{20})}{2 C_2 (C_1 + C_2)^2} \qquad (C\text{-}12)$$